DOI 10.4430/bgo00385

Free-air vertical gravity gradient modelling and its validation

Y.A. Akdoğan[1], G.O. Ahi[2] and H. Yildiz[3]

[1] *Geodesy Department, General Directorate of Mapping, Ankara, Turkey*
[2] *University of Hacettepe, Department of Geomatics Engineering, Ankara, Turkey*
[3] *Higher Technical School of Surveying, General Directorate of Mapping, Ankara, Turkey*

(Received: 30 July 2021; accepted: 12 December 2021; published online: 8 June 2022)

ABSTRACT The theoretical value of the free-air Vertical Gravity Gradient (VGG) is used when the measured or modelled VGG are not available. The errors of using the theoretical VGG become larger in rough topography and propagate into the gravimetric reductions and geoid determination. As measuring the VGG is difficult and time-consuming, the VGG can be modelled. Here, we present a VGG model developed by the 3D least-squares collocation using the remove-compute-restore method. The accuracy of the VGG model is validated over western Turkey by *in-situ* VGG measurements at 159 ground points. The results show a satisfactory agreement of about 190 Eötvös between the modelled and the measured VGG values. Moreover, the variability of the modelled VGG with respect to the topographic elevations are also investigated. At higher than 1000 m elevations, the deviation from the theoretical value becomes significant. The accuracy of the measurements improves 30 μGal when the modelled VGGs are used for the gravimetric reduction of the absolute gravity value, from the measurement point to the ground as transferred height. To conclude, instead of the theoretical VGG, the use of the VGG model is suggested for reducing the absolute gravity values particularly in rough topography.

Key words: Free-air, vertical gravity gradient, remove-compute-restore method, least-squares collocation, instrument height correction.

1. Introduction

Traditional gravimetric methods use generally only the vertical component of the gravity vector while gradiometric methods rely on all the multiple components of the gravity gradients (W_{xx}, W_{yy}, W_{zz}, W_{xy}, W_{xz}). The use of second-order derivatives of the gravitational potential, VGG (W_{zz}), in the following parts of this manuscript VGG refer to the free-air vertical gravity gradients, is of particular importance because the VGG possesses better resolution than the gravity (Li, 2001) and its signal spectral power is shifted to higher frequencies, which is more sensitive to the short-wavelength signal compared to the gravity anomaly (Wan *et al.*, 2019). Considering geophysical applications, several authors used the VGG: e.g. Álvarez *et al.* (2015) to delineate shallow density contrasts; Götze and Pail (2018) to study the boundaries of geological structures such as intrusions, faults and, in larger scales, the continental-oceanic transition at continental margins; Kim and Wessel (2011) and Sandwell *et al.* (2014) carried out investigations on the plate-tectonics; Veryaskin and McRae (2008) used the VGG for lithospheric modelling to study dynamic topography and glacial isostatic adjustment for bedrock geometry determination under

ice sheets. Considering geodetic applications, the VGG are important for the instrument height correction and the reduction of the observed gravity from the topography to the geoid (Völgyesi, 2001; Tóth *et al.,* 2006). The geoid determination is crucial as being the reference surface for height systems, useful for navigation, and crucial for large engineering projects. More clearly, the use of the theoretical VGG induces significant systematic errors in geoid determination, especially in mountainous areas, reaching up to the level of centimetres to several metres (Featherstone and Allister, 2001; Huang *et al.*, 2001; Hwang and Hsiao, 2003; Tenzer *et al.*, 2005, 2016; Santos *et al.*, 2006; Flury and Rummel, 2009; Tenzer and Vaníček, 2003; Sjöberg and Bagherbandi, 2012; Bagherbandi and Tenzer, 2013). Thus, to enhance the accuracy of the gravity reductions and the geoid computation, the analytical models that fit measured VGGs should be preferred instead of the theoretical one (Rózsa and Tóth, 2005).

The VGGs can be computed by inversion from the gravity and torsion balance measurements (Völgyesi *et al.*, 2012) or measured by terrestrial gradiometry (e.g. Simav *et al.*, 2013; Akdoğan *et al.*, 2019), airborne gradiometry (e.g. Difrancesco *et al.*, 2009), and satellite gradiometry (e.g. Rummel *et al.*, 2011; Yildiz, 2012; Yildiz *et al.*, 2017) or derived from satellite altimetry data (e.g. Wang, 2000; Minzhang *et al.*, 2014). Concerning the satellite technologies, especially the Gravity field and steady-state Ocean Circulation Explorer (GOCE) mission offers the five independent components of the spatial gravity gradients of the geopotential. The GOCE's derived gravity gradients are provided by the onboard ultra-sensitive three-axis gravity gradient gradiometer (Cesare *et al*., 2010). In satellite altimetry, one way is to transform along-track derivatives into E-W and N-S deflections of the vertical, and with the use of the Laplace equation VGG grids can be obtained (Wang, 2001; Kim and Wessel, 2016). Measuring VGGs is difficult and time-consuming as well as limited only to the accessible areas. The airborne gradiometry is expensive and needs a proper downward continuation from the flight altitude to the ground or geoid and provides lower spatial resolution than the VGG measurements.

Free-air VGG modelling has been studied by several scientists with different methods and compared with a number of *in-situ* measurements, which resulted in suggesting the use of modelled free-air VGGs instead of the theoretical (Rapp and Pavlis, 1990; Vanicek *et al.*, 2001; Rózsa and Tóth, 2005; Tenzer and Ellmann, 2009; Zhu and Jekeli, 2009; Hájková, 2011). Rózsa and Tóth (2005) have validated their results using just six measurement points. Bucha *et al.* (2016) calculated a VGG model by the summation of EIGEN-6C4 GGM model (Förste *et al.*, 2014) up to a degree of 2190, residual terrain model (RTM), derived from a high-resolution DTM (2 arcsec), and the residual from the expansion coefficients. The modelled VGG are further validated only at 20 *in-situ* VGG measurement points with a standard deviation of 279 Eötvös between the observed and the modelled values. More recently, Vajda *et al*. (2020) investigated the impact of digital elevation models with sufficient resolution and accuracy on VGG modelling and validated their results with *in-situ* measurements in prominent and rugged topography.

The novelty of this paper is estimating a new free-air VGG model using 3D least-squares collocation (LSC) by the remove-compute-restore (RCR) method. Moreover, the estimated new VGG model is validated by in total 159 *in-situ* VGG measurements. The impact of varying elevation on the modelled VGG is also studied.

The main focus of this paper is to evaluate the impact of the modelled VGGs on the reduction of the absolute gravity values from the measurement point of an absolute gravimeter to the ground level in comparison with the use of the theoretical VGG. For this part of the study, the height of the absolute gravity instrument from a ground point is arbitrarily chosen as 75 cm, which roughly corresponds to the measurement height of the Micro-g LaCoste A10 absolute gravimeter. Considering the study area, a mountainous region, the dependency and the variability

of the modelled VGGs with respect to the topographic heights is investigated.

After the first introductory part, the Section 2 elaborates the study area and the data used. Section 3 describes the 3D LSC using RCR method, used for VGG modelling. In Section 4, the validation of the modelled VGGs with the measured VGGs, the contribution of the modelled VGGs to the instrument height correction of absolute gravity measurements, and the deviation of the modelled VGGs from the theoretical VGG are presented. Finally, several conclusions are drawn in Section 5.

2. Study area and the data set

The study area is located between 36° and 42° N and 26° and 32° E in western Turkey (see Fig. 1, the study area is shown in a blue rectangle). The study area is selected based on the criteria of the availability of the densely and homogeneously distributed VGG measurements. Fig. 1 shows the locations and the spatial distribution of the VGG measurements along with the topographical heights of the study area.

The minimum and maximum heights of the study area range from 0 to 2700 m, respectively.

2.1. Gravity data

For this study, the gravity values that had been measured and compiled at 26,174 points within the scope of a national project named "The Turkish Height System Modernization and Gravity Infrastructure Recovery (2015-2020)" (Simav and Yildiz, 2019) are used. The spatial resolution of the gravity points is about 2 arcmin.

The 3D positions of the measured gravity points are estimated from the Real-Time Kinematic (RTK) observations of the continuous Global Navigation Satellite System (GNSS) network service so-called as the Continuously Operating Reference Stations - Türkiye [CORS-TR: Eren *et al.* (2009)]. The mean accuracies of the ITRF96 coordinates of the gravity points are about a few centimetres in horizontal components and better than 1 dm in vertical components (Simav and Yildiz, 2019). To convert the ellipsoidal heights of gravity points to Helmert orthometric heights, the Turkish Geoid-2003 [TG-03: Kılıçoğlu *et al.* (2005)] is used. Then, the free-air gravity anomalies at the gravity points are computed based on the GRS80 reference ellipsoid parameters (Moritz, 2000).

A total of 26,174 point-wise free-air gravity anomalies are selected lying nearest to the knots of a regular grid with a resolution of about 2 arcmin (~ 4 km at the equator). The statistical properties of the point-wise free-air gravity anomalies are given in Table 1.

Table 1 - The statistics of the point-wise free-air gravity anomalies in mGal (1 mGal = 1000 μGal).

Minimum value	Maximum value	Mean	Standard deviation
-58.14	226.45	51.12	35.40

2.2. VGG measurements

In the study area, there are pre-performed VGG measurements acquired with Scintrex CG5 and CG3 gravimeters during 2012 to 2015 (Simav *et al.*, 2013). In addition to these measurements, new VGG measurements, from 2016 till 2019, are carried out within the scope of the Turkish

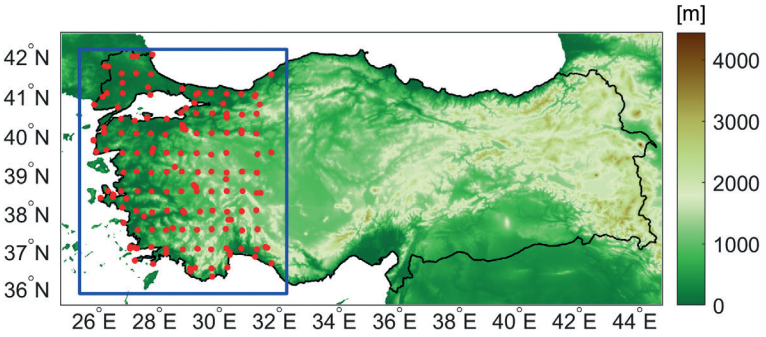

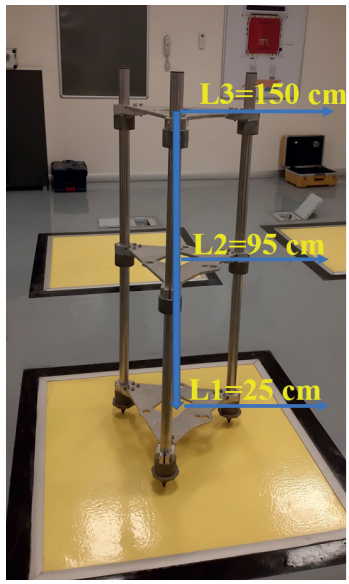

Fig. 1 - The distribution of the VGG measurements (red dots, in total: 159) over the study area (in the blue rectangle) is illustrated in the left plot. A photo of the platform, used for the measurements of VGG with relative gravimeters is shown to the right.

Height System Modernization and Gravity Infrastructure Recovery project (2015-2020). In total, there are 159 available VGG measurements (Fig. 1, left plot with red dots).

A special platform, having three measurement levels (L1 = 25 cm, L2 = 95 cm, L3 = 150 cm), is designed for the abovementioned VGG measurements. The measurements are performed at 3 measurement level with the specified order of measurements: L1 - L2 - L3 - L2 - L1 - L3 - L1- L2 - L3. In each level gravity measurements during a 60 s period are repeated 5 times for each location (see Fig. 1, right plot).

The repetition of measurements provides the computation of instrumental drift due to the transportation of the gravimeter from one location to another. The VGGs are calculated from:

$$W_{zz}^{meas.}(h_i) = \frac{g(h_i) - g(h_0)}{\Delta h} \tag{1}$$

where $g(h_i)$ and $g(h_0)$ denote the gravity at different heights, Δh the height difference, and $W_{zz}^{meas.}(h_i)$ the measured VGGs. The statistical information of the VGG measurements is given in Table 2 (covering the area of about one-third of Turkey).

The VGGs are varying between 2306 and 4283 Eötvös, with a mean value of 3116 Eötvös based on 159 VGG measurements in the study area. This suggests that the mean VGG differs about 30 Eötvös with respect to the theoretical VGG equal to 3086 Eötvös (0.3086 mGal/m = 308.6 μGal/m). The differences between the observed and the theoretical values of the VGG range from -25 to +39% indicate the necessity to consider the measured VGGs instead of the theoretical VGG values.

Table 2 - The descriptive statistics of the VGG measurements used in this study, in Eötvös.

	Minimum	Maximum	Mean formal error	Mean	Standard deviation
Total	2306	4283	19	3116	363.5

2.3. Global Geopotential Model (GGM)

To remove the effect of the global gravity field from the local measurements, the GOCO06s satellite-only GGM model, released in 2019 (maximum degree/order: 300) is used (Kvas *et al.*, 2021). The GGM derived free-air gravity anomaly (Δg^{GGM}) and GGM derived free-air VGG anomaly (T_{zz}^{GGM}) are needed for VGG modelling (Section 3.1.). The corresponding spherical harmonic coefficients for the computation of the Δg^{GGM} and T_{zz}^{GGM} were downloaded from the International Centre for Global Earth Models (ICGEM) (Sinem Ince *et al.*, 2019).

2.4. MERIT DEM

To remove the high-resolution terrain effects from the gravity field quantities, e.g. VGG and gravity anomalies, a Digital Elevation Model (DEM) is used. The removal of the topography effect is a step performed in VGG modelling. In this study, MERIT DEM (Yamazaki *et al.*, 2017) is chosen for the removal of the residual terrain model (RTM) effects (Forsberg, 1984). It represents highly accurate terrain elevations at 3 arcsec resolution (~ 90 m at the equator). Moreover, the advantage of the MERIT DEM compared to other spaceborne DEMs is the elimination of multiple errors components (e.g. absolute bias, stripe noise, speckle noise, and tree height bias) inducing the height errors compared to the other existing solutions. Mean elevation surface is obtained with an averaging process of the MERIT DEM to 0.25 arcdegree resolution.

3. Methodology

The mathematical equation of the VGG $\partial g/\partial H$ or W_{zz} can be defined as (Hwang and Hsiao, 2003; Hofmann-Wellenhof and Moritz, 2006):

$$\frac{\partial g}{\partial H} = \frac{\partial \gamma}{\partial H} + \frac{\partial \Delta g}{\partial H} \tag{2}$$

$$W_{zz} = U_{zz} + T_{zz} \tag{3}$$

where $\partial\gamma/\partial H$ or U_{zz} denote the theoretical VGG, which equals 3086 Eötvös, $\partial\Delta g/\partial H$ or T_{zz} express the VGG anomaly. T_{zz} comprises of the long-wavelength component of the VGG anomaly T_{zz}^{GGM}, the residual VGG anomaly T_{zz}^{res} and the short-wavelength of the VGG anomaly derived from the digital elevation model T_{zz}^{RTM} as follows:

$$W_{zz}^{model} = U_{ZZ} + T_{zz}^{GGM} + T_{zz}^{res.} + T_{zz}^{RTM} \tag{4}$$

3.1. Modelling the VGG

In this study, the VGG anomalies T_{zz} are first modelled at the grid points spaced as 2 by 2 arcsec. Then, the modelled VGGs, W_{zz}^{Model}, are derived by adding the theoretical VGG, U_{zz} (Eq. 4).

The computations are carried out following the RCR method. First, the gravity measurements on the Earth surface are transformed into the free-air gravity anomalies. Then, as the reduction

step, the residual free-air gravity anomalies ($\Delta g^{res.}$) are derived by reducing those calculated from the global gravity field model, representing the long-wavelength effect in addition to the topography effect calculated from RTM, representing the short wavelengths. In the computation step, the residual VGG (T_{zz}^{res}) is estimated from the residual free-air gravity anomalies ($\Delta g^{res.}$) using the 3D LSC method (Moritz, 1976; Tscherning, 2013):

$$T_{zz}^{res} = C_{T_{zz}^{res.}\Delta g^{res.}} C^{-1}_{\Delta g^{res.}\Delta g^{res.}} \Delta g^{res.} \tag{5}$$

$$\Delta g^{res.} = \Delta g^{meas.} - (\Delta g^{GGM} + \Delta g^{RTM}) \tag{6}$$

where $C_{\Delta g^{res.}\Delta g^{res.}}$ is the covariance matrix of the measurements ($\Delta g^{res.}$) and $C_{T_{zz}^{res.}\ \Delta g^{res.}}$ is the cross-covariance matrix between T_{zz}^{res} and $\Delta g^{res.}$.

Covariance functions of $C_{\Delta g^{res.}\Delta g^{res.}}$ and $C_{T_{zz}^{res.}\ \Delta g^{res.}}$ are determined by analytically modelling (Maggi *et al.*, 2006) the covariance function of the disturbing potential T ($cov(T_k, T_p)$) by the formula given in Moritz (1980):

$$cov(T_k, T_p) = \alpha \sum_{i=2}^{N} \left[\frac{R_E^2}{r_k r_p}\right]^{i+1} \sigma_i^2 P_i(cos\,\psi) + \sum_{i=N+1}^{\infty} \left[\frac{R_B^2}{r_k r_p}\right]^{i+1} \frac{A}{(i-1)(i-2)(i+4)} P_i(cos\,\psi) \tag{7}$$

where N is the degree of GGM (N = 220), σ_i^2 is the error degree-variance related to the GOCO06S GGM up to degree 220 consistent with the methodology of the quality assessment of the historical gravity data used in the Turkish Geoid Model-2020 computations (Yildiz *et al.*, 2021), R_E is the Earth mean radius, R_B is the radius of Bjerhammar sphere, ψ is the spherical distance between k and p, r_k, r_q are the radial distances from the origin, α is the scale parameter, A is the constant parameter with units of (m/s)^4.

An empirical covariance function is determined from $\Delta g^{res.}$ data using the GRAVSOFT EMPCOV program (Forsberg and Tscherning, 2008) and fitted to the analytical model in Eq. 7 by an iterative non-linear adjustment (Knudsen, 1987) using the GRAVSOFT COVFIT program (Forsberg and Tscherning, 2008) to estimate the covariance parameters of α (scale parameter), the Bjerhammar radius R_B and constant parameter A in Eq. 7.

The GGM derived gravity anomaly and VGG anomaly are calculated from the GOCO06s model coefficients up to d/o 220 as shown in Eqs. 8 and 9 (Bucha and Janák, 2014):

$$\Delta g^{GGM}(r, \varphi, \lambda) = \frac{GM}{r^2} \sum_{n=n_{min}}^{n_{max}} \left(\frac{R}{r}\right)^n (n-1) \sum_{m=0}^{n} \left(\Delta \bar{C}_{n,m} cosm\lambda + \Delta \bar{S}_{n,m} sinm\lambda\right) \bar{P}_{n,m}(sin\varphi) \tag{8}$$

$$T_{zz}^{GGM}(r, \varphi, \lambda) = \frac{GM}{r^3} \sum_{n=n_{min}}^{n_{maks}} \left(\frac{R}{r}\right)^n (n+1)(\mathrm{n}+2) \sum_{m=0}^{n} \left(\bar{C}_{n,m} cosm\lambda + \bar{S}_{n,m} sinm\lambda\right) \bar{P}_{n,m}(sin\varphi) \tag{9}$$

where r, φ, λ denote the spherical radius, latitude and longitude, respectively. n, m are the degree and order of the spherical harmonic coefficients, G is the international gravity constant, M is the Earth's mass, R is the Earth's radius, $\bar{C}_{n,m}$ $\bar{S}_m$ are the fully-normalised spherical harmonic coefficients, and $\bar{P}_{n,m}$ are the normalised Legendre functions.

The RTM method using Fast Fourier Transform (FFT) technique (Forsberg, 1984) by GRAVSOFT TC program (Forsberg and Tscherning, 2008) is used to compute the terrain-related gravity anomaly (Δg^{RTM}) and the terrain related free-air VGG anomaly (T_{zz}^{RTM}) using the digital elevation

model, MERIT DEM. In the last step, the long-wavelength and the short-wavelength components are restored to the residual VGG (Forsberg and Tscherning, 1981).

W_{zz}^{Model} are estimated using the multi-processing LSC subroutines of the GRAVSOFT software (Kaas *et al.*, 2013) i.e. GEOCOL19. Fig. 2 illustrates the processing steps to obtain the modelled VGG.

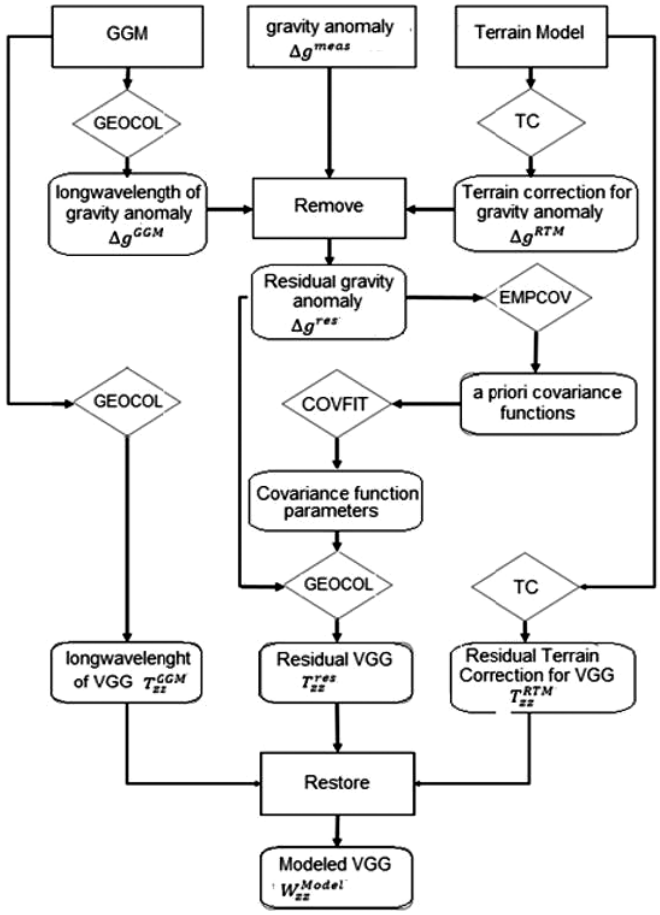

Fig. 2 - The flow chart for the modelled VGG estimation using the GRAVSOFT software (Forsberg and Tscherning, 2008; Kaas *et al.*, 2013).

4. Results and analysis

4.1. Validating the modelled VGG with the measured VGG

In this section, the modelled VGGs are compared with the measured VGGs to validate the accuracy achieved. Fig. 3a shows the modelled VGGs on the elevation contour map created from MERIT DEM at 2'×2'grid points and Fig. 3b represents the differences between the measured and modelled VGGs at the VGG measurement points. Table 3 presents the statistics of the modelled and measured VGGs. According to Fig. 3a and Table 3, modelled VGGs at 2'×2' grid points are

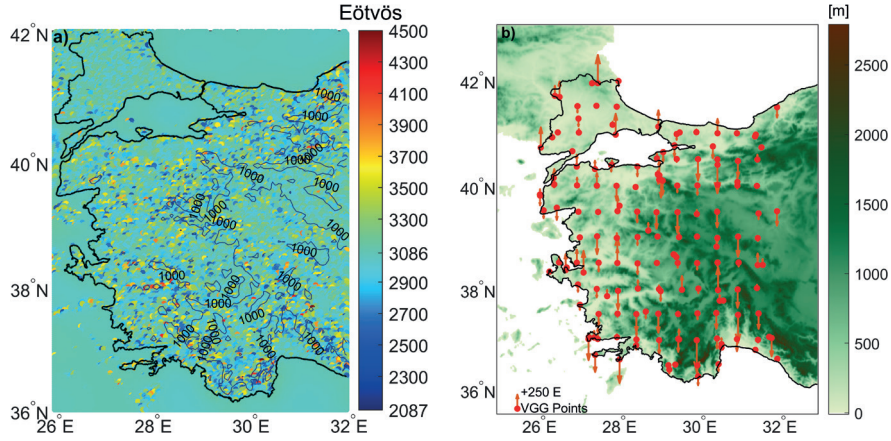

Fig. 3 - Modelled VGG at 2'×2' grid points estimated using the LSC method in Eötvös (a). MERIT DEM (min: 0 m, max: 2700 m) contour lines are plotted in blue. Differences between the measured and the modelled VGG at VGG measurement points in Eötvös (b).

varying between 2087 Eötvös and 4500 Eötvös with a mean of 3092 Eötvös. The differences between the theoretical and the modelled VGGs are found within -32% and +46%, which are very close to the values given in Section 2.2 -25% to +39%.

The differences between the modelled and the measured VGGs, have a standard deviation, which is around 190 Eötvös. This relatively small difference ±190 Eötvös, is better than the results obtained in the available literature (Rózsa and Tóth, 2005; Bucha *et al.*, 2016). The differences ranging in ±190 Eötvös between the modelled and the measured VGGs has been calculated using the VGG measurements.

Table 3 - The descriptive statistics of the measured and the modelled VGG of this study in Eötvös.

Type of Data	Minimum	Maximum	Mean	Standard deviation
Modelled	2087	4500	3092	208.8
Modelled-Measured	-566	458	-39	188.9

4.2. A case study of using the modelled VGGs for reducing the absolute gravity measurements from the gravimeter reference point to the ground point

As well known by geodesists and geophysicists, the absolute gravimetric measurements are assumed to be observed at the instrumental height, which refers to gravimetric reference point inside the vessel of the gravimeter. The measurements must be reduced from the gravimeter reference point to the ground level (Repanić *et al.*, 2015). The reduction (correction) of measured gravity values from the instrumental height to the ground level is generally performed with the theoretical VGG value and can be calculated as:

$$g(h_0) = g(h_i) + W_{zz} * \Delta h \tag{10}$$

where $g(h_0)$ is the reduced gravity at the ground point, $g(h_i)$ is gravity measured at the reference point of the (absolute) gravimeter, W_{zz} denotes the theoretical or modelled VGG value, Δh denotes the vertical distance between the gravimeter reference point and the ground point, which is fixed to 75 cm (in accordance with the A10 absolute gravimeter).

Table 4 - The descriptive statistics of the gravity correction (Eq. 10) differences in μGal due to the reduction of the measured gravity for 75 cm height difference when the measured or the modelled VGG are used.

	Minimum	Maximum	Mean	Standard deviation
Theoretical-Measured	-90	58	-2	27
Modelled-Measured	-42	34	-3	14

According to Table 4, the results clearly show that the use of the theoretical VGG causes errors reach to a value of about 90 μGal while the use of the modelled VGGs result in much smaller errors up to about 40 μGal due to the reduction of the measured gravity for 75 cm height difference.

4.3. The deviation of the modelled VGGs from the theoretical VGG with respect to elevation

To further investigate the elevation dependency of the deviation, modelled VGG values are separated into five groups determined by grid point elevations (see Table 5). The limits of the height increments of the groups are from 0 to 500, 500 to 1000, 1000 to 1500, 1500 to 2000, and 2000 to 2700 m, respectively. Table 5 shows the statistics of the modelled VGGs at different elevation intervals. The theoretical VGG value is 3086 Eötvös, as introduced previously, and the deviation expresses the difference of the modelled VGGs from this theoretical value.

This study shows that the modelled VGG values are close to the theoretical VGG value in flat areas (0-500 m, 500-1000 m). However, in areas higher than 1000 m, the VGG values exhibit large deviations from the theoretical value. These results reveal that in mountainous countries such as Turkey, the use of the theoretical VGG instead of the modelled or the measured VGG may result in large errors, e.g. in the height reductions of the gravity measurements.

Table 5 - The descriptive statistics of the modelled VGG at different height increments in Eötvös.

	Height increments	Minimum	Maximum	Standard deviation	Mean	Deviation from the theoretical VGG
Modelled VGG	0-500 (m)	2086	4039	151	3069	17
	500-1000 (m)	2150	4333	258	3094	8
	1000-1500 (m)	2124	4428	248	3123	37
	1500-2000 (m)	2330	4467	311	3277	191
	2000-2700 (m)	2680	4500	345	3474	388

5. Conclusions

In this study, a VGG model is estimated from the 3D LSC using the RCR method. The comparison of modelled VGGs with the *in-situ* VGG measurements show a good agreement with a standard deviation of the differences of about 190 Eötvös. Only the error due to LSC prediction seems to affect the results, regarding the errors induced in the model from the geopotential model as well as the DTM used.

Using the modelled VGGs, instead of the theoretical VGG for the instrumental height

correction, causes a decrease of the gravity reduction errors from about 90 to 40 μGal. Considering the deviations of the modelled VGGs from the theoretical VGG with the elevation, at low-lying areas, up to 1000 m sea level height, the modelled VGGs are found to be close to the theoretical VGG values. However, at higher than 1000 m elevations, the deviation from the theoretical value becomes significant at the level of about 250-350 Eötvös in standard deviation. This result suggests that using the modelled VGGs for instrumental height reduction at such elevations would improve the accuracy of the gravity networks. This result also infers that if the VGG cannot be measured at each gravity point, in mountainous areas like Turkey, instead of the theoretical VGG, at least the modelled VGGs should be used.

Acknowledgments. This gravity and VGG data used in this study are provided by the General Directorate of Mapping Turkey. The gravity and VGG data were measured and compiled under the framework of the Turkish Height System Modernization and Gravity Infrastructure Recovery (2015-2020) project, conducted by the General Directorate of Mapping Turkey with the cooperation of the General Directorate of Mineral Research and Exploration (MTA), Turkey Petroleum, TUBITAK Marmara Research Centre (MAM) and TUBITAK National Metrology Institute. Turkish Height System Modernization and Gravity Infrastructure Recovery (2015-2020) is funded by the Department of Strategy and Budget of the Presidency of the Republic of Turkey. This research is a product of the MSc. thesis of YAA supervised by GOA and co-supervised by HY. The authors thank Dr. Kamil Teke for his valuable comments on this study.

REFERENCES

Akdoğan Y.A., Yildiz H. and Ahi G.O.; 2019: *Evaluation of global gravity models from absolute gravity and vertical gravity gradient measurements in Turkey*. Meas. Sci. Technol., 30, 115009, doi: 10.1088/1361-6501/ab2f1c.

Álvarez O., Nacif S., Spagnotto S., Folguera A., Gimenez M., Chlieh M. and Braitenberg C.; 2015: *Gradients from GOCE reveal gravity changes before Pisagua Mw = 8.2 and Iquique Mw = 7.7 large megathrust earthquakes*. J. South Am. Earth Sci., 64, 273-287, doi: 10.1016/j.jsames.2015.09.014.

Bagherbandi M. and Tenzer R.; 2013: *Geoid-to-quasigeoid separation computed using the GRACE/GOCE global geopotential model GOCO02S - A case study of Himalayas and Tibet*. Terr. Atmos. Oceanic Sci. J., 24, 59-68, doi: 10.3319/TAO.2012.09.17.02(TT).

Bucha B. and Janák J.; 2014: *A MATLAB-based graphical user interface program for computing functionals of the geopotential up to ultra-high degrees and orders: efficient computation at irregular surfaces*. Comput. Geosci., 66, 219-227, doi: 10.1016/j.cageo.2014.02.005.

Bucha B., Janák J., Papčo J. and Bezděk A.; 2016: *High-resolution regional gravity field modelling in a mountainous area from terrestrial gravity data*. Geophys. J. Int., 207, 949-966, doi: 10.1093/gji/ggw311.

Cesare S., Aguirre M., Allasio A., Leone B., Massotti L., Muzi D. and Silvestrin P.; 2010: *The measurement of Earth's gravity field after the GOCE mission*. Acta Astronaut., 67, 702-712, doi: 10.1016/j.actaastro.2010.06.021.

Difrancesco D., Grierson A., Kaputa D. and Meyer T.; 2009: *Gravity gradiometer systems - Advances and challenges*. Geophys. Prospect., 57, 615-623, doi: 10.1111/j.1365-2478.2008.00764.x.

Eren K., Uzel T., Gulal E., Yildirim O. and Cingoz A.; 2009: *Results from a comprehensive Global Navigation Satellite System test in the CORS-TR network: case study*. J. Surv. Eng., 135, 10-18, doi: 10.1061/(asce)0733-9453(2009)135:1(10).

Featherstone W. and Allister N.; 2001: *Estimation of Helmert orthometric heights using digital barcode levelling, observed gravity and topographic mass-density data over part of the Darling scarp, western Australia*. Geomatics Res. Australas., 75, 25-52.

Flury J. and Rummel R.; 2009: *On the geoid-quasigeoid separation in mountain areas*. J. Geod., 83, 829-847, doi: 10.1007/s00190-009-0302-9.

Forsberg R.; 1984: *A study of terrain reductions, density anomalies and geophysical inversion methods in gravity field modelling.* Department of Geodetic Science and Surveying, Ohio State University, Columbus, OH, USA, Report 355, 134 pp.

Forsberg R. and Tscherning C.C.; 1981: *The use of height data in gravity field approximation by collocation.* J. Geophys. Res., 86, 7843-7854, doi: 10.1029/JB086iB09p07843.

Forsberg R. and Tscherning C.C.; 2008: *GRAVSOFT, an overview manual for the Geodetic Gravity Field Modelling Programs*. DTU Space, Kongens Lyngby, Denmark, 68 pp.

Förste C., Bruinsma S.L., Abrikosov O., Lemoine J.-M., Marty, Jean Charles., Flechtner F., Balmino G., Barthelmes F. and Biancale R.; 2014: *EIGEN-6C4, the latest combined global gravity field model including GOCE data up to degree and order 2190 of GFZ Potsdam and GRGS Toulouse*. GFZ Data Services, Potsdam, Germany, WWW document, doi: 10.5880/ICGEM.2015.1.

Götze H.J. and Pail R.; 2018: *Insights from recent gravity satellite missions in the density structure of continental margins - With focus on the passive margins of the South Atlantic*. Gondwana Res., 53, 285-308, doi: 10.1016/j.gr.2017.04.015.

Hájková J.; 2011: *Local geoid determination based on airborne gravity data*. Stud. Geophys. Geod., 55, 515-528, doi: 10.1007/s11200-011-0031-4.

Hofmann-Wellenhof B. and Moritz H.; 2006: *Physical Geodesy*. Springer-Verlag, Wien, Austria, 405 pp., doi: 10.1007/b139113.

Huang J., Vanícek P., Pagiatakis S.D. and Brink W.; 2001: *Effect of topographical density of geoid in the Canadian Rocky Mountains*. J. Geod., 74, 805-815, doi: 10.1007/s001900000145.

Hwang C. and Hsiao Y.S.; 2003: *Orthometric corrections from leveling, gravity, density and elevation data: a case study in Taiwan*. J. Geod., 77, 279-291, doi: 10.1007/s00190-003-0325-6.

Kaas E., Sørensen B., Tscherning C.C. and Veicherts M.; 2013: *Multi-processing least squares collocation: applications to gravity field analysis*. J. Geod. Sci., 3, 219-223, doi: 10.2478/jogs-2013-0025.

Kim S.S. and Wessel P.; 2011: *New global seamount census from altimetry-derived gravity data*. Geophys. J. Int., 186, 615-631, doi: 10.1111/j.1365-246X.2011.05076.x.

Kim S.S. and Wessel P.; 2016: *New analytic solutions for modeling vertical gravity gradient anomalies*. Geochem. Geophys. Geosyst., 17, 1915-1924, doi: 10.1002/2016GC006263.

Kılıçoğlu A., Firat O. and Demir C.; 2005: *Observations and methods used in the computation of new Turkish geoid (TG-03)*. In: Kaya A., Yalçınkaya M. and Yıldırım F. (eds), Geoid and Vertical Datum Workshop, Scientific Meeting of Turkish National Geodesy Commission, Karadeniz Technical University, Trabzon, Turkey, pp. 53-76.

Knudsen; 1987: *Estimation and modelling of the local empirical covariance function using gravity and satellite altimeter data*. Bull. Géod., 61, 145-160, doi: 10.1007/BF02521264.

Kvas A., Brockmann J.M., Krauss S., Schubert T., Gruber T., Meyer U., Mayer-Gürr T., Schuh W-D., Jäggi A. and Pail R.; 2021: *GOCO06s - A satellite-only global gravity field model*. Earth Syst. Sci. Data, 13, 99-118, doi: 10.5194/essd-2020-192.

Li X.; 2001: *Vertical resolution: gravity versus vertical gravity gradient*. The Leading Edge, 20, 901-904, doi: 10.1190/1.1487304.

Maggi A., Migliaccio F., Reguzzoni M. and Tselfes N.; 2006: *Combination of ground gravimetry and GOCE data for local geoid determination: a simulation study*. In: Proc. 1st International Symposium of the International Gravity Field Service (IGFS), Istanbul, Turkey, 6 pp.

Minzhang H., Jiancheng L., Hui L. and Lelin X.; 2014: *Bathymetry predicted from vertical gravity gradient anomalies and ship soundings*. Geod. Geodyn., 5, 41-46, doi: 10.3724/sp.j.1246.2014.01041.

Moritz H.; 1976: *Covariance functions in least-squares collocation*. Department of Geodetic Science, Ohio State University, Columbus, OH, USA, Report 240, 88 pp.

Moritz H.; 1980: *Global covariance models.* In: Advanced physical geodesy, Abacus Press, Royal Tunbridge Wells, UK, Part B, Chapter 23, 181-195 pp.

Moritz H.; 2000: *Geodetic reference system 1980*. J. Geod., 74, 128-133, doi: 10.1007/s001900050278.

Rapp R.H. and Pavlis N.K.; 1990: *The development and analysis of geopotential coefficient models to spherical harmonic degree 360*. J. Geophys. Res., 95, 21885-21911, doi: 10.1029/jb095ib13p21885.

Repanić M., Kuhar M. and Malović I.; 2015: *High precision vertical gravity gradient determination in Croatia*. Acta Geod. Geophys., 50, 151-171, doi: 10.1007/s40328-015-0102-z.

Rózsa S. and Tóth G.; 2005: *Prediction of vertical gravity gradients using gravity and elevation data*. In: Sansò F. (ed), A Window on the Future of Geodesy, Proc. International Association of Geodesy Symposia, Springer, Berlin - Heidelberg, Germany, Vol 128, pp. 344-349, doi: 10.1007/3-540-27432-4_59.

Rummel R., Yi W. and Stummer C.; 2011: *GOCE gravitational gradiometry*. J. Geod., 85, 777-790, doi: 10.1007/s00190-011-0500-0.

Sandwell D.T., Müller R.D., Smith W.H.F., Garcia E. and Francis R.; 2014: *New global marine gravity model from CryoSat-2 and Jason-1 reveals buried tectonic structure*. Sci., 346, 65-67, doi: 10.1126/science.1258213.

Santos M.C., Vaníček P., Featherstone W.E., Kingdon R., Ellmann A., Martin B.A., Kuhn M. and Tenzer R.; 2006: *The relation between rigorous and Helmert's definitions of orthometric heights*. J. Geod., 80, 691-704, doi: 10.1007/s00190-006-0086-0.

Simav M. and Yildiz H.; 2019: *Evaluation of EGM2008 and latest GOCE-based satellite only global gravity field models using densified gravity network: a case study in south-western Turkey*. Boll. Geof. Teor. Appl., 60, 49-68, doi: 10.4430/bgta0255.

Simav M., Yıldız H., Direnç A. and Türkezer A.; 2013: *Terrestrial gravity measurements towards Turkish height system modernization*. In: Abstracts EGU General Assembly Conference, Wien, Austria, Vol. 15, p. 12260,

Sinem Ince E., Barthelmes F., Reißland S., Elger K., Förste C., Flechtner F. and Schuh H.; 2019: *ICGEM - 15 years of successful collection and distribution of global gravitational models, associated services, and future plans*. Earth Syst. Sci. Data, 11, 647-674, doi: 10.5194/essd-11-647-2019.

Sjöberg L.E. and Bagherbandi M.; 2012: *Quasigeoid-to-geoid determination by EGM08*. Earth Sci. Inf., 5, 87-91, doi: 10.1007/s12145-012-0098-7.

Tenzer R. and Vaníček P.; 2003: *Correction to Helmert's orthometric height due to actual lateral variation of topographical density*. Rev. Bras. Cartogr., 55, 44-47.

Tenzer R. and Ellmann A.; 2009: *On evaluation of the mean gravity gradient within the topography*. In: Sideris M.G. (ed), Observing our Changing Earth, Proc. International Association of Geodesy General Assembly (2007), Springer, Berlin-Heidelberg, Germany, pp. 253-261, doi: 10.1007/978-3-540-85426-5_30.

Tenzer R., Vaníček P., Santos M., Featherstone W.E. and Kuhn M.; 2005: *The rigorous determination of orthometric heights*. J. Geod., 79, 82-92, doi: 10.1007/s00190-005-0445-2.

Tenzer R., Hirt C., Novák P., Pitoňák M. and Šprlák M.; 2016: *Contribution of mass density heterogeneities to the quasigeoid-to-geoid separation*. J. Geod., 90, 65-80, doi: 10.1007/s00190-015-0858-5.

Tóth G., Földvári L., Tziavos I.N. and Ádám J.; 2006: *Upward/downward continuation of gravity gradients for precise geoid determination*. Acta Geod. Geophys. Hungarica, 41, 21-30, doi: 10.1556/AGeod.41.2006.1.3.

Tscherning C.C.; 2013: *Geoid determination by 3D least-squares collocation*. In: Sansò F. and Sideris M. (eds), Geoid Determination, Lecture Notes in Earth System Sciences, Springer, Berlin-Heidelberg, Germany, Vol. 110, pp. 311-336, doi: 10.1007/978-3-540-74700-0_7.

Vajda P., Zahorec P., Papčo J., Carbone D., Greco F. and Cantarero M.; 2020: *Topographically predicted vertical gravity gradient field and its applicability in 3D and 4D microgravimetry: Etna (Italy) case study*. Pure Appl. Geophys., 177, 3315-3333, doi: 10.1007/s00024-020-02435-x.

Vanicek P., Janák J. and Huang J.; 2001: *Mean vertical gradient of gravity*. In: Sideris M. (ed), Gravity, Geoid and Geodynamics 2000, International Association of Geodesy Symposia, Springer, Berlin-Heidelberg, Vol. 123, pp. 259-262, doi: 10.1007/978-3-662-04827-6_43.

Veryaskin A. and McRae W.; 2008: *On combined gravity gradient components modelling for applied geophysics*. J. Geophys. Eng., 5, 348-356, doi: 10.1088/1742-2132/5/3/010.

Völgyesi L.; 2001: *Local geoid determination based on gravity gradients*. Acta Geod. Geophys. Hungarica, 36, 153-162, doi: 10.1556/AGeod.36.2001.2.3.

Völgyesi L., Dobróka M. and Ultmann Z.; 2012: *Determination of vertical gradients of gravity by series expansion based inversion*. Acta Geod. Geophys. Hungarica, 47, 233-244, doi: 10.1556/AGeod.47.2012.2.11.

Wan X., Ran J. and Jin S.; 2019: *Sensitivity analysis of gravity anomalies and vertical gravity gradient data for bathymetry inversion*. Mar. Geophys. Res., 40, 87-96, doi: 10.1007/s11001-018-9361-8.

Wang Y.M.; 2000: *Predicting bathymetry from the Earth's gravity gradient anomalies*. Mar. Geod., 23, 251-258, doi: 10.1080/01490410050210508.

Wang Y.M.; 2001: *GSFC00 mean sea surface, gravity anomaly, and vertical gravity gradient from satellite altimeter data*. J. Geophys. Res. C: Oceans, 106, 31167-31174, doi: 10.1029/2000jc000470.

Yamazaki D., Ikeshima D., Tawatari R., Yamaguchi T., O'Loughlin F., Neal J.C., Sampson C.C., Kanae S. and Bates P.D.; 2017: *A high-accuracy map of global terrain elevations*. Geophys. Res. Lett., 44, 5844-5853, doi: 10.1002/2017GL072874.

Yildiz H.; 2012: *A study of regional gravity field recovery from GOCE vertical gravity gradient data in the Auvergne test area using collocation*. Stud. Geophys. Geod., 56, 171-184, doi: 10.1007/s11200-011-9030-8.

Yildiz H., Forsberg R., Tscherning C.C., Steinhage D., Eagles G. and Bouman J.; 2017: *Upward continuation of Dome-C airborne gravity and comparison with GOCE gradients at orbit altitude in east Antarctica*. Stud. Geophys. Geod., 61, 53-68, doi: 10.1007/s11200-015-0634-2.

Yildiz H., Simav M., Sezen E., Akpinar İ., Akdogan Y.A., Cingoz A. and Akabali O.A.; 2021: *Determination and validation of the Turkish Geoid model-2020 (TG-20).* Bull. Geophys. Oceanogr., 62, 495-512, doi: 10.4430/bgo00345.

Zhu L. and Jekeli C.; 2009: *Gravity gradient modeling using gravity and DEM*. J. Geod., 83, 557-567, doi: 10.1007/s00190-008-0273-2.

Corresponding author: Yunus Aytaç Akdoğan
Geodesy Department, General Directorate of Mapping
Tip. Fakultesi Caddasi, Dikimevi, Ankara, Turkey
Phone: +90 312 595 2246; e-mail: yunusaytac.akdogan@harita.gov.tr